Protease sensing using nontoxic silicon quantum dots

Author:
Cheng, X; McVey, BFP; Robinson, AB; Longatte, G; O'Mara, PB; Tan, VTG; Thordarson, P; Tilley, RD; Gaus, K; ... Gooding, Justin

Publication details:
Journal of Biomedical Optics
v. 22
Chapter No. 8
Medium: Print
pp. 087002 - 087002
1083-3668 (ISSN); 1560-2281 (ISSN)

Publication Date:
2017-08-01

Publisher DOI:
https://doi.org/10.1117/1.JBO.22.8.087002

Protease Sensing Using Nontoxic Silicon Quantum Dots

Xiaoyu Cheng,[ab] Benjamin F.P. McVey,[a] Andrew B. Robinson,[a] Guillaume Longatte,[a] Peter B. O'Mara,[a] Vincent T. G. Tan,[a] Pall Thordarson,[a] Richard D. Tilley,[a] Katharina Gaus,[b] J. Justin Gooding*[a]

a School of Chemistry, Australian Centre for NanoMedicine, ARC Centre of Excellence in Convergent Bio-Nano Science and Technology, The University of New South Wales, Sydney, NSW 2052, Australia.

b EMBL Australia Node in Single Molecule Science, School of Medical Sciences, ARC Centre of Excellence in Advanced Molecular Imaging, The University of New South Wales, Sydney, NSW 2052, Australia.

Abstract. Herein is presented a proof-of-concept study of protease sensing which combines nontoxic silicon quantum dots (SiQDs) with Förster resonance energy transfer (FRET). The SiQDs serve as the donor, and an organic dye as the acceptor. The dye is covalently attached to the SiQDs using a peptide linker. Enzymatic cleavage of the peptide leads to changes in FRET efficiency. The combination of interfacial design and optical imaging presented in this work opens new opportunities for using nontoxic silicon quantum dots relevant to intracellular sensing and imaging.

Keywords: quantum dots, silicon, biosensor, FRET, self-assembled monolayer

***Corresponding author:** Prof. J. Justin Gooding**,** E-mail: justin.gooding@unsw.edu.au

1. Introduction

For a biosensor to be used in physiological conditions, ideally the information from the sensor should be obtained non-invasively and the sensor should not influence regular biological processes. Far-field optical imaging fulfils the first criteria. Colloidal quantum dots combined with far-field imaging are ideal for biosensing due to their small size, tunable surface properties and unique optical signatures. However, the fact that many optically active colloidal nanoparticles contain toxic heavy metal elements has potentially compromised their ability to fulfil the second criteria of not perturbing the environment they are designed to monitor.(1) This has led to growing interest in developing quantum dots made with materials of low toxicity, represented by group IV elements such as carbon and silicon.(2, 3) Currently, ultrasmall fluorescent colloidal silicon quantum dots (SiQDs) of a few nanometers in size have been shown to be benign *in vivo* and as a

consequence they have been applied in imaging, sensing, real-time cell tracking and specific destruction of cancer cells, and drug delivery.(4-12)

Förster resonance energy transfer (FRET) is one of the methods by which quantum dots can be used in biosensing.(13-17) This can be by using the quantum dots as either the acceptor or the donor.(18) The initial example of quantum dots FRET protease sensor was reported more than a decade ago,(13) but to date this concept has not been shown with nontoxic silicon quantum dots.(10, 19) The difficulty with using SiQDs in biosensing has been surface modification such that silicon oxide is prevented.(20, 21) Preventing silicon oxide is important as silicon is an indirect bandgap semiconductor, which means the optical properties of SiQDs are sensitive to surface properties.(22)

(Scheme 1)

The purpose of this paper is to show that SiQDs can be used as donors for FRET based biosensors for measuring protease activity where the acceptor is an organic dye. As shown in Scheme 1, the SiQD FRET sensors were synthesized in a stepwise manner to demonstrate the sensing capability of SiQDs in protease sensing. The final biosensor was composed of peptide linkers attached to a SiQD donor at one end and attached to an acceptor dye DY485 at the other (referred to as SiQD-RGDC-DY485 sensor). Cleavage of a peptide by a protease enzyme resulted in removal of the dye and a diminution in FRET efficiency. Protease enzymes are the family of enzymes that performs proteolysis. They are overexpressed in most cancers, and proteolytic activity has been one of the most important sensing targets for cancer diagnosis.(23) Overexpression of protease enzymes is also associated with infection, cholesterol regulations, apoptosis and necrosis.(23) In this study trypsin was used as a model protease. Trypsin is a serine protease produced mainly in the pancreas as a proenzyme trypsinogen.(24)

2. Methods and Materials

Chemicals and materials

Silicon tetrabromide ($SiBr_4$), tetraoctylammoniabromide (TOAB), lithium aluminium hydride ($LiAlH_4$, 1.0 M THF solution), 1,7-octadiene, Hoescht 33258, 10×trypsin EDTA (1 mM) stock were purchased from Sigma-Aldrich and were used as received unless otherwise stated. RGDC peptide was purchased from Genscript. The fluorescent dye DY485-NHS was obtained from Dyomics. Dry solvents were obtained by passing through a PURE-SOLV (Innovative Technology) solvent purification system with water content below 15 ppm.

Synthesis and purification of 1,7-octadiene passivated silicon quantum dots

Hydrogen terminated SiQDs were prepared in accordance with a published method(8, 25-27). In brief, all experiments were performed under Ar using a standard Schlenk line set-up. In a typical experiment, 100 μL of $SiBr_4$, (0.8×10^{-3} mole) and 1.5 g TOAB (2.7×10^{-3} mole) were dissolved in 100 mL toluene in a 250 mL three-neck flask. The mixture was sonicated for 20 min. An excess amount of $LiAlH_4$ (6×10^{-3} mole, excess) was then added, and the mixture was further stirred and sonicated for 45 min. The reaction was then quenched with dry ethanol until no bubble seen and kept under argon.

Alkene terminated SiQDs were prepared by reacting 1,7-octadiene with hydrogen terminated SiQDs and then purified via size exclusion chromatography. The hydrogen terminated SiQDs obtained in the previous step were transferred to a 250 mL quartz reaction vessel (ACE Glass Inc.) via a cannula needle under Ar. For each hydrosilylation reaction, 4 mL of octadiene was added, and the mixture was treated with UV (254 nm) for 15 h. After the reaction, all solvent and unreacted alkene was evaporated under reduced pressure and elevated temperature, with the crude

product obtained as pale-yellow oil. To the mixture was then added water (3 × 20 mL) and hexane (3 × 20 mL). The hexane layer was extracted, and was passed through PVDF membrane with 0.45 μm pore size. To further purify octadiene passivated SiQDs, size-exclusion chromatography was used. All of the hexane was evaporated and particles were re-suspended in 3 mL of toluene. Bio-Beads SX bead was used as the stationary phase and toluene was used as eluent with no pressure applied. Only fractions that showed blue photoluminescence under a UV lamp were collected. The column with washed with twice the amount of the beads volume after purification.

Preparation of SiQDs-DY485 FRET Conjugates

For a typical thiol-ene 'click' reaction on the alkene functionalized SiQDs, the solvent containing 5 mg of SiQDs-octadiene dispersion was first evaporated, and then was added with 1 mL of peptide (sequence: N'-RGDC-C' DMSO or DMF solution at concentration of 5 mg/mL. The mixture was treated under UV (4 × 8 W) for 5 hours to allow sufficient coupling of the thiol-ene click reaction to complete. The mixture was then dialyzed with Tube-O-Dialyzer (1.5k MWCO, G-Biosciences) in 1 × PBS at 4 ºC for 24 hours with buffer replaced every eight hours. The sample was then recovered, and DY485-NHS was added in desired concentration for 3 hours to allow coupling reaction to complete.

Characterization of morphology and optical properties of SiQDs

The size and morphology of the synthesized SiQDs was characterized by transmission electron microscopy (TEM) and dynamic light scattering (DLS) measurements. TEM measurements were performed on a Philip CM 200 microscope operated at 200kV. All TEM images were visualized without staining. DLS measurements were performed on a Brookhaven 90 Plus Instrument.

Measurements were performed at 25 ºC and intensity mean was plotted versus the size distribution. Experimental parameters used: scan time: 50; buffer condition: hexane for hydrophobic surface nanoparticles and PBS for hydrophilic surface nanoparticles; scattering angle: 173 degrees. Surface functionalization of silicon quantum dots was characterized by FT-IR spectroscopy. FT-IR measurements were performed on an Avatar 320 FT-IR spectrometer. Measurements were done by dropping 10 μL of concentrated silicon quantum dot dispersion onto a pellet premade by grinding powder of KBr. H-NMR measurements were performed on a Bruker 300MHz instrument to confirm the purity of synthesized nanoparticles. The optical properties of silicon quantum dots were characterized by UV-Vis and fluorescence spectroscopy. UV-Vis spectra were recorded on a Cary-50 UV-Vis spectrometer and fluorescence spectra measured on a Cary-Eclipse Fluorescence spectrometer.

MTT toxicity assay

An MTT (3-[4,5-dimethylthiazol-2-yl]-2,5 diphenyl tetrazolium bromide) assay (Sigma-Aldrich) was performed to evaluate cellular toxicity of SiQDs. HeLa cells were cultured to 70 – 80% confluence in a 96-well plate prior to experiment. For each 20μL of SiQDs was added to each well and incubated for 24 hours. After the incubation, the MTT reagent (5 mg/mL) was reconstituted in PBS, and was added in an equal volume. The cells were further incubated for 2 to 3 hours. After the incubation period, the resulting formazan crystals were dissolved by adding equal volume of DMSO to the original culture medium volume. Upon fulling dissolving the crystals, the absorption measurements were performed using a FLUOstar fluorescence plate reader (BMG Labtech) at 570 nm and background at 690 nm.

3. Results and Discussions

3.1 Characterization of surface modified silicon quantum dots

(Figure 1)

The SiQDs were characterized extensively prior to utilizing the SiQD-RGDC-DY485 biosensors. TEM results indicated that the obtained nanoparticles were spherical in shape and relatively monodisperse with an average size of the silicon cores of 3.4 ± 0.7 nm (

Figure **1**A). High resolution TEM images revealed lattice fringes matching the (220) lattice spacing of silicon. Dynamic light scattering measurements showed that hydrodynamic size of the SiQDs was 5.4 ± 0.6 nm (

Figure **1**B). After conjugation of the peptide there was a slight increase in SiQDs size, with the small peak measured as 7.2 ± 1.2 nm. (

Figure **1**C). Greater amounts of aggregation were also observed after the modification process. For successful fabrication of the SiQDs FRET donor, we highlight the importance of nanoparticle purification. After each surface modification steps, nanoparticles showed expected signatures with FT-IR measurements. (

Figure **1**E) In particular, bands at 1600 cm^{-1} at 3055 cm^{-1} were due to the distal alkene on the surface, whereas peaks at 3400 cm^{-1} and 1700 cm^{-1} were evidence for the successful grafting of the peptides. With the protocol used, typically ~10 mg of purified SiQDs were obtained, while adding more precursors led to aggregated by products and particles were no longer monodisperse. The progress of the surface modification could also be monitored by the solvent phases in which the SiQDs could be dispersed and from their luminescence (Figure 1D). When modified with 1,7-octadiene, the nanoparticles were only dispersible in nonpolar solvents such as hexane and naturally only the luminescence of the SiQDs was observed. After attachment of the hydrophilic peptide onto the surface, the SiQDs became dispersible in water. Further modification with dye

molecules resulted in the SiQD-RGDC-DY485 sensor remaining in aqueous solution but now the luminescence changed from blue to orange upon UV excitation of 365 nm. This color change reflected FRET from the SiQD donor to the DY485 acceptor with its characteristic emission. The optical characteristics of the SiQD-RGDC-DY485 sensors were described in a conference proceedings, as is also indicated in

Figure **1**F.(28)

The organic dye acceptor used in this study, DY485, was chosen primarily because it has a large Stokes shift of ~85 nm (**Error! Reference source not found.**A) which provides minimal overlap between the emissions of the SiQD donor and the acceptor. Hence emission from donor channel can be observed without interference from the acceptor. Furthermore the absorption of DY485 exhibits good overlap with the emission peak of SiQDs as needed for a good FRET donor/acceptor pair.(13) With the donor-acceptor pair presented herein, the Förster radius was calculated to be ~3.2 nm, where the spacing between the dye and the nanoparticle was estimated to be ~2.5 nm. This calculation was determined from the surface of the SiQDs as emission from SiQDs is has been shown previously to be most likely interface dominated.(22, 27-29)

3.2 *Sensor Performance*

(Figure 2)

Coupling the dye to the SiQDs resulted in FRET occurring as shown visually in Figure 1D. The spectral changes of the SiQD-RGDC-DY485 as a function of time as the acceptor dye is attached is shown in Figure 2A. What is apparent from this figure is the growth on the acceptor emission as a function of time as expected for with more dye being attached with longer coupling times. Less expected was the only minor decrease in the donor peak during the coupling reaction. A closer inspection for the photoluminescence trend at the donor channel (Figure 2B) showed that

photoluminescence intensity ratio dropped immediately after the addition of the dye, where after the intensity remained fairly stable with less than 10% variation over the remaining reaction time. We attribute this observation to two factors. The first being that silicon is an indirect bandgap semiconductor as in contrast to conventional quantum dots which are typically made from direct bandgap materials. This has led to lower quantum yield and also a strong impact of surface properties over photophysics of the particles, as seen by us and other groups previously.(12, 22, 30, 31) The second factor is that since we did not purify the conjugate after dye coupling, the drop of signal at the donor channel could be predominated by strong absorption of the dye. Note this cannot be attributed to nonspecific adsorption of the dye because a control experiment with hydrolyzed DY485 which did not increase the acceptor channel signal (2E). The response of the sensor to the addition of trypsin is shown in Figure 2B and C. Upon addition of the trypsin, the FRET efficiency to the accept dye decreased as indicated by the diminution in intensity of the emission peak at 550 nm. This result suggests that trypsin has cleaved the peptide linkage between the SiQD and the dye and hence less dye is within appreciable FRET distance. Note again the donor emission peak is insensitive to the extent of FRET. The timescale over which this cleavage occurs us shown in Figure 2B and F. The fact that the sensor is specific toward trypsin is shown in Figure 2F where the addition collagenase (100 μg/mL) or MMP2 (140 μg/mL) under same experimental conditions resulted in no change in luminescence and hence no cleavage of the peptide linker.

3.3 Kinetic analysis of enzyme activity

For protease sensing, the FRET conjugate was treated with trypsin, which cleaves at the C terminus of glycine of the peptide sequence (Figure 2 B and C). With an increasing amount of enzyme added, the respective photoluminescence measurements indicated a more significant change of

FRET response until a maximum change was reached at ~460 μg/mL (Figure 2D). This was in comparison to the control group treated with phosphate buffer saline (PBS), which did not show any significant change in photoluminescence throughout the experiment; thus showing the change in FRET response was due to the cleavage of the peptide. The reaction kinetics of the enzymatic cleavage as depicted in Figure 2D was then investigated. With the step-wise surface modification strategy used, the substrate concentration and nanoparticle/ligand ratios were not known.(32, 33) For this reason, a modified approach for studying the surface reaction kinetics of our system was needed. To do this we used I_d/I_a as a function of enzyme reaction time, which was then fitted with a global non-linear regression model using an integrated form of the Michaelis-Menten equation using Lambert function and known enzyme concentration.(34)

More specifically, protease reactions progress as:

$$E + S \rightleftarrows ES \rightarrow E + product \quad \text{(Eq. 9)}$$

With the rate equation given as:

$$v = -\frac{d}{dt}[S](t) = \frac{k_{cat}[E_0][S](t)}{K_m + [S](t)} \text{ (Eq. 10)}$$

Since in our case the substrate concentration is unknown while the enzyme concentration is known, which is opposite to the situation for conventional studies, the analysis of our data is based on direct integration of the Michaelis-Menten equation using the Lambert *W* function as shown by Schnell and Mendoza:(34)

$$[\mathrm{S}]_t = K_m W_0\left(\frac{[\mathrm{S}]_0}{K_m} e^{\left(\frac{[\mathrm{S}]_0 - V_m t}{K_m}\right)}\right) \text{ (Eq. 11)}$$

Here W_0 stands for the Lambert W equation which can be solved by accurate straightforward numerical approaches via *Matlab*. The maximum enzymatic turnover frequency: k_{cat}, is simply the maximum rate achieved by the system; V_m, divided by $[E]_0$, such that

$$k_{cat} = \frac{V_m}{[\mathrm{E}]_0} \rightarrow V_m = k_{cat}[\mathrm{E}]_0 \text{ (Eq. 12)}$$

Here, the total enzyme concentration $[E]_0$ is known but not the total substrate concentration $[S]_0$. Therefore, by inserting Eq. 12 in Eq. 11, we obtain

$$[S]_t = K_m W_0\left(\frac{[S]_0}{K_m} e^{\left(\frac{[S]_0 - k_{cat}[E]_0 t}{K_m}\right)}\right) \text{ (Eq. 13)}$$

An important assumption is made here, such that within the measurements range I_A is a linear function of the substrate density on the surface of SiQDs. This comes from the fact that FRET induced fluorescence changes at the donor channel due to FRET is very small. Indeed, the application of the quasi-steady state approximation to the donor excited channel gives its concentration expression called $[D^*]$ as a function of the total donor concentration $[D]$ and the different rate constants (k_{exc} for the excitation, k_F for the relaxation by fluorescence emission, k_{FRET} for the relaxation by FRET to the acceptor and k_i all other relaxation pathway (thermal relaxation, and all other quenching process) and [S] the substrate concentration (product of nanoparticle concentration and of number of substrate by nanoparticle):

$$[D^*] = [D]\frac{k_{exc}}{k_{exc}+k_F+[S]k_{FRET}+\sum_{i=1}^{N} k_i} \text{ (Eq. 14)}$$

As the fluorescence is proportional to the rate of relaxation by fluorescence emission (first order reaction with$[D^*]$ as reactant and k_F as rate constant), the fact that little change in the donor channel is observed as a function of the acceptor concentration suggests that $[A]k_{FRET} \ll k_{exc} + k_F + \sum_{i=1}^{N} k_i$. In other words the donor quenching observed is dominated by factors other than FRET. This let us rewrite the last expression of the excited donor concentration which is independent of the substrate concentration:

$$[D^*] = [D]\frac{k_{exc}}{k_{exc}+k_F+\sum_{i=1}^{N} k_i} \text{ (Eq. 15)}$$

Similarly, the excited acceptors concentration can be expressed as:

$$[S^*] = [S]\frac{k_{FRET}[D^*]}{k_{FRET}[D^*]+k_{F,S}+\sum_{i=1}^{N} k_{i,S}} \text{ (Eq. 16)}$$

If we assume that the intensity in the acceptor channel is proportional to $[S^*]$, the independence of $[D^*]$ with [S] gives that I_a is proportional to $[S]$. However a final background value has to be added into the modelling. Using this assumption we can now relate Eq. 16 directly to the observed (I_d/I_a) ratio at any given time $(I_d/I_a)_t$, assuming a background final value of $(I_d/I_a)_\infty$ and by defining the molar concentration response of (I_d/I_a) as $\square[(I_d/I_a)]$:

$$\left(\frac{I_d}{I_a}\right)_t = \frac{\left(\frac{I_d}{I_a}\right)_\infty}{1+\varepsilon\left(\frac{I_d}{I_a}\right)\left[K_m W_0\left(\frac{[S]_0}{K_m} e^{\left(\frac{[S]_0 - k_{cat}[E]_0 t}{K_m}\right)}\right)\right]} \quad \text{(Eq. 17)}$$

This equation was then used as the basis of a global fit all five (I_d/I_a) curves below

(Figure 3)

By this method, an estimate of both k_{cat}/K_m = 1.06 $mM^{-1}s^{-1}$, and the total substrate concentration $[S]_0$ = 0.48 μM was obtained. It should be noted that with the method devised was not possible to obtain independent values of K_m and k_{cat}, but only their ratio as the results suggested [E]>>[ES]. The fitting also suggested the value of k_{cat}/K_m was about 3-5 times lower than reported value for trypsin catalyzed proteolytic cleavage of a longer peptide conjugate on conventional quantum dots.(33)

3.4 Nanoparticle toxicity

Figure 4

To test nanoparticle toxicity, we performed MTT toxicity experiments with the SiQDs donor and the FRET conjugate *in vitro* using HeLa cells. The particles were incubated with the cells overnight at different concentrations, and no apparent toxic effect was seen for particle amount up to 256 μg/mL compared with the control group, where only phosphate buffer saline was applied. The

results were consistent with what previously reports showing no toxic effect of silicon quantum dots.(26, 27, 35, 36)

4. Conclusions

In summary, we report the first proof-of-concept study of FRET protease sensing with quantum dots made from a non-toxic material, crystalline silicon. This was achieved by a combination of materials synthesis, interfacial design and advanced far-field imaging techniques. Mechanistic study revealed that the surface reaction follows Michaelis-Menten kinetics model. The general applicability of wet chemistry and thiol based surface modification strategy presented allow a simple way of preparing colloidal silicon quantum dots sensors for immobilizing target molecules onto the surface, and the use of microscopic method suggested measurements can be performed in cellular contexts. The concepts brought by this paper aim to bring new opportunities of bio-applications using nontoxic quantum dots in sensing and in general.

5. Disclosure

The authors declare no competing financial interests.

6. Acknowledgement

We acknowledge the generous financial support from the Australian Research Council Centre of Excellence in Convergent Bio-Nano Science and Technology (CE140100036; J.J.G. and P.T.), ARC Australian Laureate Fellowship (FL150100060; J.J.G.), ARC Centre of Excellence in Advanced Molecular Imaging (CE140100011; K.G.), Senior Research Fellowship from the National Health and Medical Research Council of Australia (APP1059278; K.G.).

7. References

1. M. Bottrill, and M. Green, "Some aspects of quantum dot toxicity," *Chem Commun* **47**(25), 7039-7050 (2011).
2. M. Dasog et al., "Silicon Nanocrystals and Silicon-Polymer Hybrids: Synthesis, Surface Engineering, and Applications," *Angew Chem Int Ed Engl* **55**(7), 2322-2339 (2016).
3. X. Cheng et al., "Colloidal silicon quantum dots: from preparation to the modification of self-assembled monolayers (SAMs) for bio-applications," *Chem Soc Rev* **43**(8), 2680-2700 (2014).
4. Y. Su et al., "In vivo distribution, pharmacokinetics, and toxicity of aqueous synthesized cadmium-containing quantum dots," *Biomaterials* **32**(25), 5855-5862 (2011).
5. J. A. Kelly et al., "Size-dependent reactivity in hydrosilylation of silicon nanocrystals," *J Am Chem Soc* **133**(24), 9564-9571 (2011).
6. C. M. Hessel et al., "Synthesis of Ligand-Stabilized Silicon Nanocrystals with Size-Dependent Photoluminescence Spanning Visible to Near-Infrared Wavelengths," *Chem Mater* **24**(2), 393-401 (2012).
7. F. Erogbogbo et al., "Biocompatible luminescent silicon quantum dots for imaging of cancer cells," *ACS Nano* **2**(5), 873-878 (2008).
8. J. H. Warner et al., "Water-soluble photoluminescent silicon quantum dots," *Angew Chem Int Ed Engl* **44**(29), 4550-4554 (2005).
9. R. K. Baldwin et al., "Room temperature solution synthesis of alkyl-capped tetrahedral shaped silicon nanocrystals," *J Am Chem Soc* **124**(7), 1150-1151 (2002).
10. Y. Su, X. Ji, and Y. He, "Water-Dispersible Fluorescent Silicon Nanoparticles and their Optical Applications," *Advanced Materials* **28**(47), 10567-10574 (2016).
11. C. Song et al., "Peptide-Conjugated Fluorescent Silicon Nanoparticles Enabling Simultaneous Tracking and Specific Destruction of Cancer Cells," *Anal Chem* **87**(13), 6718-6723 (2015).
12. X. Cheng et al., "One-pot synthesis of colloidal silicon quantum dots and surface functionalization via thiol-ene click chemistry," *Chem Commun (Camb)* **48**(97), 11874-11876 (2012).
13. I. L. Medintz et al., "Self-assembled nanoscale biosensors based on quantum dot FRET donors," *Nat Mater* **2**(9), 630-638 (2003).
14. V. Palomo et al., "3,4-Dihydroxyphenylalanine Peptides as Nonperturbative Quantum Dot Sensors of Aminopeptidase," *ACS Nano* **10**(6), 6090-6099 (2016).
15. F. Erogbogbo et al., "Energy transfer from a dye donor to enhance the luminescence of silicon quantum dots," *Nanoscale* **4**(16), 5163-5168 (2012).
16. M. Locritani et al., "Silicon Nanocrystals Functionalized with Pyrene Units: Efficient Light-Harvesting Antennae with Bright Near-Infrared Emission," *J Phys Chem Lett* **5**(19), 3325-3329 (2014).
17. A. M. Dennis et al., "Quantum dot-fluorescent protein FRET probes for sensing intracellular pH," *ACS Nano* **6**(4), 2917-2924 (2012).
18. W. R. Algar et al., "Quantum Dots as Simultaneous Acceptors and Donors in Time-Gated Förster Resonance Energy Transfer Relays: Characterization and Biosensing," *Journal of the American Chemical Society* **134**(3), 1876-1891 (2012).

19. C. M. Gonzalez, and J. G. C. Veinot, "Silicon nanocrystals for the development of sensing platforms," *J. Mater. Chem. C* **4**(22), 4836-4846 (2016).
20. S. Ciampi, J. B. Harper, and J. J. Gooding, "Wet chemical routes to the assembly of organic monolayers on silicon surfaces via the formation of Si-C bonds: surface preparation, passivation and functionalization," *Chemical Society Reviews* **39**(6), 2158-2183 (2010).
21. F. Hua, M. T. Swihart, and E. Ruckenstein, "Efficient Surface Grafting of Luminescent Silicon Quantum Dots by Photoinitiated Hydrosilylation," *Langmuir* **21**(13), 6054-6062 (2005).
22. M. Dasog et al., "Chemical insight into the origin of red and blue photoluminescence arising from freestanding silicon nanocrystals," *ACS Nano* **7**(3), 2676-2685 (2013).
23. C. Cordovilla, and T. M. Swager, "Strain release in organic photonic nanoparticles for protease sensing," *J Am Chem Soc* **134**(16), 6932-6935 (2012).
24. A. Schuchert-Shi, and P. C. Hauser, "Peptic and tryptic digestion of peptides and proteins monitored by capillary electrophoresis with contactless conductivity detection," *Anal Biochem* **387**(2), 202-207 (2009).
25. R. D. Tilley et al., "Micro-emulsion synthesis of monodisperse surface stabilized silicon nanocrystals," *Chem Commun (Camb)* **0**(14), 1833-1835 (2005).
26. A. Shiohara et al., "Chemical reactions on surface molecules attached to silicon quantum dots," *J Am Chem Soc* **132**(1), 248-253 (2010).
27. X. Cheng et al., "Versatile "click chemistry" approach to functionalizing silicon quantum dots: applications toward fluorescent cellular imaging," *Langmuir* **30**(18), 5209-5216 (2014).
28. X. Cheng et al., "Colloidal silicon quantum dots: from preparation to the modification of self-assembled monolayers for bioimaging and sensing applications," *Proc. SPIE* 100780O-100780O-100710 (2017).
29. Q. Li et al., "Silicon Nanoparticles with Surface Nitrogen: 90% Quantum Yield with Narrow Luminescence Bandwidth and the Ligand Structure Based Energy Law," *ACS Nano* **10**(9), 8385-8393 (2016).
30. M. Dasog et al., "Size vs surface: tuning the photoluminescence of freestanding silicon nanocrystals across the visible spectrum via surface groups," *ACS Nano* **8**(9), 9636-9648 (2014).
31. X. Cheng et al., "Enhancing Quantum Dots for Bioimaging using Advanced Surface Chemistry and Advanced Optical Microscopy: Application to Silicon Quantum Dots (SiQDs)," *Adv Mater* **27**(40), 6144-6150 (2015).
32. S. A. Diaz et al., "Probing the kinetics of quantum dot-based proteolytic sensors," *Anal Bioanal Chem* **407**(24), 7307-7318 (2015).
33. W. R. Algar et al., "Proteolytic activity at quantum dot-conjugates: kinetic analysis reveals enhanced enzyme activity and localized interfacial "hopping"," *Nano Lett* **12**(7), 3793-3802 (2012).
34. S. Schnell, and C. Mendoza, "Enzymological considerations for a theoretical description of the quantitative competitive polymerase chain reaction (QC-PCR)," *J Theor Biol* **184**(4), 433-440 (1997).
35. Y. Zhong et al., "Large-Scale Aqueous Synthesis of Fluorescent and Biocompatible Silicon Nanoparticles and Their Use as Highly Photostable Biological Probes," *Journal of the American Chemical Society* (2013).
36. Y. Zhong et al., "Microwave-Assisted Synthesis of Biofunctional and Fluorescent Silicon Nanoparticles Using Proteins as Hydrophilic Ligands," *Angewandte Chemie International Edition* **51**(34), 8485-8489 (2012).

TOC Graphic

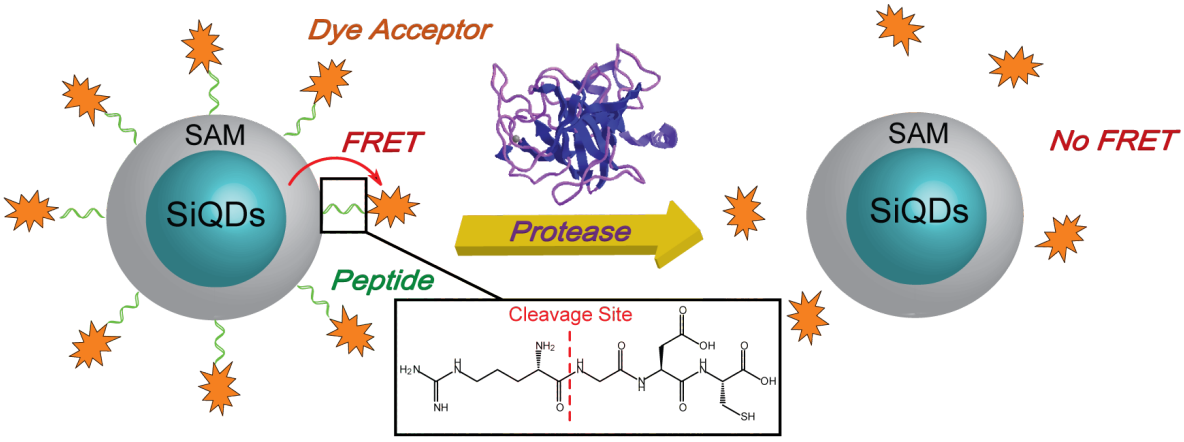
Dye Acceptor
SAM
SiQDs
FRET
Protease
Peptide
Cleavage Site
SAM
SiQDs
No FRET

Figure Captions

Scheme 1 Schematic of the fabrication of the FRET protease sensor based on silicon quantum dots. As synthesized SiQDs were modified with 1,7-octadiene using UV light followed by attachment of a peptide sequence RGDC where the free thiol on the cysteine couples to the distal alkene on the monolayer modified SiQD. The dye molecule DY485-NHS was then attached to the free amine at the N-terminus of the peptide sequence. Protease activity is then determined by the change in photoluminescence (PL) as the peptide is cleaved by the enzyme.

Figure 1 Characterization of size and surfaces of SiQDs used as the FRET donors. (A) Representative transmission electron microscopy (TEM) images and high resolution (HR-TEM) images showing the spherical morphology and lattice fringes of nanoparticles synthesized (B-C) Dynamic light scattering measurements confirming the narrow size distribution of alkene (B) and peptide conjugated (C) silicon quantum dots. (D) Picture showing the fluorescence of the nanoparticles in different phases obtained from each surface conjugation step. The nanoparticles were dispersed in solvents containing hexane (top layer) or Milli-Q water (bottom layer) under direct excitation using a 365 nm UV lamp (E) FT-IR of surface modified SiQDs. (F) Spectral overlay between SiQDs and DY485 as also indicated in (28)

Figure 2 Sensor performance. (A) Change of PL with time upon addition of DY485 (20 μM). An immediate drop of PL was seen after the addition of the dye acceptor, while the donor peak remained largely stable throughout the rest of the reaction. Excitation wavelength: 350 nm. (B) Typical Id/Ia trend monitored over the entire experiment. (C) Change of PL upon the addition of trypsin at 460 μg/mL. (D) Enzymatic response of the SiQDs protease sensor at different trypsin concentrations. (E) Reaction with hydrolyzed DY485 showed a drop in the donor channel but no increase of intensity in the acceptor channel (F) Enzyme specificity study using collagenase (100 μg/mL) and matrix metalloproteinases 2 (MMP2, 140 μg/mL) which showed no effect on the FRET signal in contrast to clear change for trypsin (115 μg/mL). Experiments were performed with 20 μM of DY485 with excitation wavelength of 350 nm.

Figure 3 Enzyme kinetics. The enzymatic response of the SiQDs protease sensor showing the raw data (blue stars) vs. fitted rate curves based on a global non-linear fit to the integrated Michaelis-Menten equations with panel A-E corresponding to the different trypsin protease concentration shown. The results from the fitting process are also shown in the lower right corner.

Figure 4 Nanoparticle toxicity. MTT toxicity test after 24 hours incubation with SiQDs in reference to control group treated with phosphate buffer saline. The results suggest no acute toxicity for nanoparticle concentration up to 256 μg/mL.

Biographies

Xiaoyu Cheng
Xiaoyu Cheng graduated with BSc (Hons) with first class honours in Chemistry in 2010 from the Australian National University. In 2015 he obtained a Ph.D in Chemistry from the University of New South Wales, supervised by Prof. Justin Gooding. The focus of his Ph.D research is the preparation and surface modification of silicon quantum dots for bioimaging and sensing applications. His research interests are in the bio-nano interfaces, biophotonics and nanophotonics.

Benjamin F.P. McVey
Benjamin F. P. McVey completed his PhD at the University of New South Wales in 2017 under the supervision of Professors Richard Tilley and J. Justin Gooding. His PhD focused on the synthesis and development of low toxicity nanoparticle bioimaging agents. He is currently interested in the synthesis and biomedical application of both metal and semiconductor nanoparticles.

Andrew B. Robinson
Andrew received his BS in Chemistry from the University of New South Wales and is currently a PhD Candidate at the University of New South Wales. His research experience is predominantly in peptide chemistry and supramolecular systems specialising in hydrogels, self-assembly, and the analysis of the biocompatibility of materials for medical application.

Guillaume Longatte
Guillaume Longatte is a post-doctoral research follow in the Smart Materials and Surfaces research group since October 2015 under the guidance of Professor Gooding. His researched is focused on photochemistry with molecules of biological interest like proteins or DNA. Before that, he did his Ph.D. in Christian Amatore's group in Paris. Previously he got his master of electrochemistry at *Université Pierre et Marie Curie* in 2012.

Peter B. O'Mara
Peter O'Mara graduated with a BSc (Hons) in with first class honours in Chemistry (2016) from the University of New South Wales. He is now reading for a PhD with Professors Gooding and Tilley on the synthesis, surface modification and bio-applications of quantum dots.

Vincent T. G. Tan
Vincent. T. G. Tan graduated from the University of New South Wales with his Bachelor of Medicinal Chemistry, developing responsive polymeric nanoparticles for drug delivery. He is currently completing his Ph.D in Chemistry under the supervision of Professor J. Justin Gooding, developing 3D printable bio-inks for cell cultures. Vincent is interested in looking for new pathways of creating self-healing printable inks for biomedical applications such as spheroid growth.

Pall Thordarson
Prof. Pall Thordarson (Palli). BSc. Iceland (1996), PhD Sydney (2001). Appointed Senior Lecturer at UNSW (2007-2012), promoted to Assoc. Prof 2013 and Professor in 2017. With over 100 publications, his research interest range from Nanomedicine to Supramolecular and Systems Chemistry. He has received a number of awards including the 2012 Le Fèvre Memorial Prize

from the Australian Academy of Science for outstanding basic research in Chemistry by a Scientist under the age of 40.

Richard D. Tilley
Professor Richard Tilley is the Director of Electron Microscope Unit at UNSW. His research is focused on the solution synthesis of nanoparticles for applications ranging from catalysis to biomedical imaging. He graduated with a Masters of Chemistry from Oxford University. He did his PhD in the Department of Chemistry, University of Cambridge, UK, after which he was a Postdoctoral Fellow for two years at the Toshiba basic R&D Center, Japan.

Katharina Gaus
Scientia Professor Katharina Gaus is an NHMRC Senior Research Fellow at the University of New South Wales, Head of the EMBL Australia Node in Single Molecule Science and Deputy Director of the ARC Centre of Excellence in Advanced Molecular Imaging. She received her PhD from the University of Cambridge in 1999 and has led an independent research group since 2005. Her group investigates signal transduction processes in T lymphocytes with advanced fluorescence microscopy approaches.

J. Justin Gooding
Scientia Professor Justin Gooding is an Arc Australian Laureate Fellow at the University of New South Wales, Co-Director of the Australian Centre for NanoMedicine and the New South Wale Smart Sensing Network. He received her DPhil from the University of Oxford in 1994 and has led an independent research group since 1999. His group specializes in surface modification for a range of applications including biosensing drug delivery, biomaterials and electron transfer studies.